Luminescence Imaging

DOI: 10.1002/ange.201404948

Image-Contrast Technology Based on the Electrochemiluminescence of Porous Silicon and Its Application in Fingerprint Visualization**

*Jie Tan, Linru Xu, Tong Li, Bin Su, and Jianmin Wu**

Abstract: *The electrochemiluminescence (ECL) of porous silicon (pSi) has attracted great interest for its potential application in display technology and chemical sensors. In this study, we found that pSi with a different surface chemistry displayed an apparently different dynamic ECL process. An image-contrast technology was established on the basis of the intrinsic mechanism of the ECL dynamic process. As a proof of principle, the visualization of latent fingerprints (LFPs) and in situ detection of TNT in fingerprints was demonstrated by using the ECL-based image-contrast technology.*

The construction of electrochemiluminescence (ECL) sensors from nanomaterials has made great progress in recent years.[1] Among the nanomaterials used, semiconductor nanocrystals constitute a major class of ECL emitters. However, for display technology or imaging analysis, an integrated semiconductor with a large surface is usually required. ECL from silicon anodes in contact with various electrolytes was first reported in 1960.[2] More recently, ECL of porous silicon (pSi) has attracted great interest for its potential application in display technology and chemical sensors.[3] High ECL efficiencies were observed for a cell with a pSi/liquid junction owing to the superior contact of the electrolyte solution with the porous layer.[4] Strong ECL emission can be generated by applying a low voltage on the pSi/liquid-junction cell. However, in all cases reported so far, the emission was short-lived and unstable, and could not be restored once it had faded. These shortcomings severely hinder the application of ECL-based pSi sensors. Usually, ECL emitted by pSi is based on a regular dynamic process, which involves activation, strong emission, and fading.[5] In the present study, we found that pSi with a different surface chemistry displayed an apparently different dynamic ECL process. As in the case of photoluminescence (PL) on pSi,[6] there are several possible explanations for the different dynamic ECL process of pSi with this different surface chemistry. Some kinds of chemicals adsorbed on the pSi surface may just block the electrochemical reaction on the pSi surface, thus resulting in a retarded activation process, whereas some chemical species may act as electron donors or acceptors, thus leading to the quenching[6a–c] or enhancement[6d] of ECL. On the basis of our understanding of the intrinsic mechanism of the dynamic ECL process, an image-contrast technology is proposed herein. The contrast in ECL intensity between different surface chemistries on the same pSi surface can produce a clear optical image on the chip. Consequently, visualization of the chemical pattern with high resolution is possible. As a proof of principle, the visualization of latent fingerprints (LFPs) impressed on a pSi chip was demonstrated by using the ECL-based image-contrast technology. A fingerprint is an impression left by the friction ridges of a human finger. Usually, fingerprints consist of perspiration, natural secretion residues, and exogenous components from the environment.[7] Some secretions or exogenous chemicals remaining on a fingertip will inevitably be transferred to any object that comes into contact with the fingertip. Therefore, impressions of fingerprints on a pSi surface may leave behind a unique spatially resolved chemical pattern, which can be visualized by the ECL-based image-contrast technology.

Porous Si was obtained by anodization of a boron-doped silicon wafer (resistivity: 0.5–1.2 $m\Omega\,cm^{-1}$) with a [100] crystal orientation in an electrolyte mixture of aqueous hydrofluoric acid (48% by mass, Alatin Corp.) and ethanol in a volume ratio of 4:1 (see the Supporting Information). An electrochemical cell with a three-electrode system was designed for ECL imaging (Figure 1 A).[8] The freshly etched pSi chip was used as the working electrode (WE), and an Ag/AgCl electrode and a platinum wire placed above the pSi chip as the reference (RE) and counter electrode (CE), respectively. A cyclic voltammogram of pSi (see Figure S1 D in the Supporting Information) showed that the current decreased continuously upon repeated scanning of the potential between −0.1 and +1.0 V (vs. Ag/AgCl), thus indicating

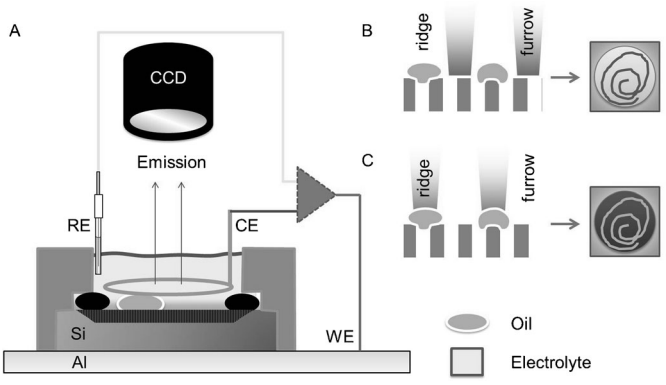

Figure 1. A) ECL imaging system. B,C) Image-contrast strategy for visualizing LPFs in the negative (B) and positive mode (C).

[*] J. Tan, L. Xu, T. Li, Prof. B. Su, Prof. J. Wu
Department of Chemistry
Institution of Microanalytical Systems, Zhejiang University
Hangzhou, 310058 (China)
E-mail: wjm-st1@zju.edu.cn

[**] This research is supported by the National Science Foundation of China (Grant No. 21275218).

Supporting information for this article is available on the WWW under http://dx.doi.org/10.1002/anie.201404948.

that the chemical reaction took place on the pSi surface. Diffuse reflectance FTIR spectroscopy (see Figure S2) revealed that the intensity of the IR peak at 2117 cm^{-1} corresponding to the Si–H_x bonds decreased with the potential-scanning cycle, whereas another IR peak at 2258 cm^{-1} grew significantly.[9] The latter peak arises from the O-Si-H_x bonds, as well as bonds with other electronegative ligands. SEM images of the pSi surface before (see Figure S1 A) and after cyclic-voltammetry measurement (see Figure S1 B) indicate that the silicon pore size increased, probably owing to the partial oxidation and dissolution of pSi during the ECL process. ECL intensity generated on pSi is not proportional to the voltammetric current (see Figure S1 C). The pSi showed a weak ECL signal during the initial scanning cycle and the highest ECL intensity was observed after several scanning cycles (about 20 cycles), thus inferring that an activation step is needed.

On the basis of these observations, the anodic ECL may arise from the injection of electrons from Si–H bonds into the conduction band (CB) of silicon through surface oxidation, as described by the following chemical equation:

$$Si{-}H_{(surface)} + H_2O + h^+_{(VB)} \rightarrow Si{-}OH_{(surface)} + 2\,H^+_{(aq)} + e^-_{(CB)} \quad (1)$$

The weak ECL intensity observed during the initial stage may be attributed to the low quantum yield of the recombination of injected electrons in the CB and holes in the valence band (VB). After partial oxidation, the intensity of ECL increased steadily as a result of the high quantum yield of recombination between the newly formed surface states (Si-OH) and the VB (Figure 2). In further potential-scanning cycles, the ECL intensity gradually faded owing to the depletion of Si–H bonds on the pSi surface. The low density of Si–H bonds leads to a decrease in the number of electrons injected into the surface states, thereby decreasing the ECL intensity. Accordingly, we can conclude that the ECL intensity greatly depends on the ratio of Si–H and Si–OH bonds on the pSi surface. High ECL intensity can only occur when the number of Si–H and Si–OH bonds is comparable. A lower density of Si-H or Si-OH bonds does not favor ECL. Therefore, ECL generated on pSi undergoes a regular dynamic process, which includes activation, strong emission, and fading.

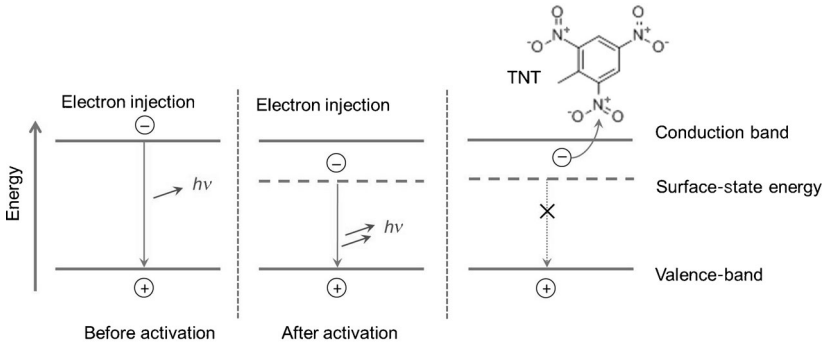

Figure 2. Mechanism of ECL activation and quenching by a TNT molecule in a p-type-pSi/liquid cell.

Relevant studies have found that PL of porous Si can be irreversibly quenched by trinitrotoluene (TNT), which is a typical kind of molecule with strong electron-withdrawing ability.[10] A similar quenching phenomenon was also observed when TNT was adsorbed on pSi (see Figure 3 A–C). To quantify the quenching effect, the captured ECL images were processed with the ImageJ2x software. The gray values of the quenched area and background can be obtained and the quenching factor (Q) is calculated from the following equation:

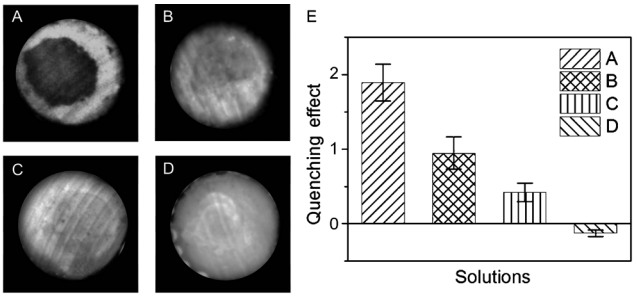

Figure 3. A–D) ECL images showing the quenching effect induced by TNT at different concentrations. A solution of TNT in methanol (5 μL) was dropped on a porous silicon chip, which was then dried and brought into contact with the electrolyte (1 M KNO_3), and a potential of 0.8 V was applied. An ECL image of the pSi surface was then recorded. Investigated concentrations of TNT in methanol: 100 (A), 10 (B), 1 (C), and 0 μg mL^{-1} (D). E) Quenching factor in (A–D).

$$Q = (G_{pSi} - G_{TNT})/G_{pSi} \quad (2)$$

in which G_{TNT} denotes the gray value of the pSi with adsorbed TNT molecules and G_{pSi} the gray value of the pSi background. The Q value displays an almost linear relationship with the logarithm of the TNT concentration, whereas the solvent (methanol) has no quenching effect on ECL intensity (Figure 3 E). On the basis of the gray-value calculation, the detection limit ($S/N > 3$) for TNT molecules is around 1 ppm. By increasing the image contrast with image-processing software, the sensitivity can be further improved. The ECL-quenching phenomenon and image-contrast measurement thus form the basis for constructing a simple and inexpensive chemical sensor device. The possible mechanism of ECL quenching is illustrated in Figure 2. Upon TNT adsorption, electrons in the surface state of pSi will transfer to TNT molecules owing to their strong electron-withdrawing ability.

On the basis of the observed quenching effect and its mechanism, we can conclude that the dynamic process of ECL emitted by pSi can be perturbed by adsorbed molecules, in analogy with the known effect of surface chemistry on the PL intensity of pSi.[6a–c] We believed that pSi with different

surface chemistry could display different dynamic processes of ECL as well. To confirm this assumption, three types of chemicals were adsorbed on the pSi surface. Among them, oil was selected as a surface blocker that can prevent contact between electrolytes and the pSi surface. TNT and tripropylamine (TPA)[5] were employed as an electron acceptor and donor, respectively. The ECL generated on the TPA-adsorbed pSi chip had an overall higher intensity than that on the unmodified pSi chip (Figure 4). The maximum ECL

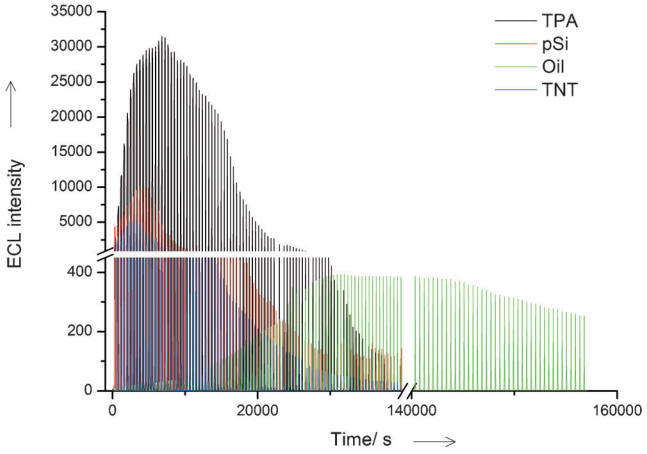

Figure 4. Real-time ECL intensity of pSi with different surface environments: pSi pretreated with a solution of TPA in methanol (10 $\mu g\,mL^{-1}$, 5 μL; black curve), freshly etched pSi (red curve), pSi pretreated with a solution of oil in methanol (10 $\mu g\,mL^{-1}$, 5 μL; green curve), and pSi pretreated with a solution of TNT in methanol (10 $\mu g\,mL^{-1}$, 5 μL; blue curve). > The ECL measurements were performed in 1 M KNO_3 as the electrolyte of the pSi/liquid cell, and the voltage of pSi was cycled from −0.1 to +1.0 V (vs. Ag/AgCl) at a scan rate of 0.1 $V\,min^{-1}$.

intensity of the TPA-adsorbed pSi was around three times as high as that of the bare pSi chip, thus showing a significant enhancement effect of TPA. In contrast, ECL intensity on the TNT-adsorbed pSi chip was almost reduced to half of that on the bare pSi chip, thus indicating a quenching effect of TNT on the whole ECL dynamic process. The porous silicon surface covered with oil displayed a much slower ECL activation process because oil could hinder the contact of porous silicon with the electrolyte and consequently block the electrochemical reaction on the pSi surface. Afterwards, the ECL intensity recovered, probably owing to the dissolution of oil during anodic voltammetric scanning. Thus, the whole ECL dynamic process on the oil-covered pSi was retarded. All results confirmed well our assumption that the ECL dynamics of pSi are sensitive to its surface chemistry. On the basis of this mechanism, the selective detection of different compounds is possible. To clarify whether the pSi-based ECL sensor was selective toward compounds with a similar structure, solutions of TNT, nitrobenzene, *p*-nitrotoluene, and toluene were dropped on different zones of a patterned porous silicon chip. The results (see Figure S3) indicated that the ECL quenching effect is significantly related to the electron-withdrawing ability of the analytes. Among them, TNT displayed the largest quenching effect, followed by *p*-nitrotoluene, nitrobenzene, and toluene. The solvent (methanol) even displayed an ECL-enhancing effect, which is similar to the result shown in Figure 3.

On the basis of our understanding of the intrinsic mechanism of the dynamic ECL process, we proposed an ECL-based image-contrast technology for visualizing chemical patterns on the pSi surface. The idea is somewhat similar to that at the heart of previous studies on the PL of pSi,[11] but the ECL-based technology may have much higher sensitivity and resolution because ECL is more sensitive to surface chemistry and generated on a dark background. To assess whether a chemical pattern on pSi can be clearly displayed with the ECL-based image-contrast technology, we dipped a stamp of the Zhejiang University (ZJU) logo in a solution of nitrobenzene (10 $\mu g\,mL^{-1}$ in methanol) and then impressed it on the surface of the pSi chip. After drying, the ECL image was recorded with a CCD camera. The ECL image of the logo was clearly visualized as a negative image, since the ECL intensity in the area with adsorbed nitrobenzene was quenched (Figure 5). The resolution of the ECL image was

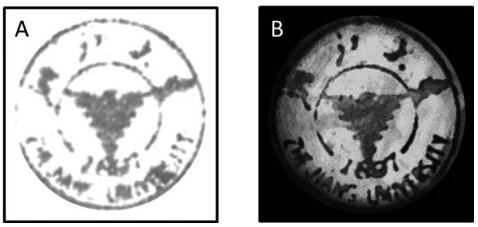

Figure 5. A) Photograph and B) ECL image of a stamp of the ZJU logo. The pattern of the logo on paper was stamped with an ink pad. ECL imaging of the ZJU logo stamped with nitrobenzene as a solution in methanol (10 $\mu g\,mL^{-1}$) on porous silicon. The ECL measurement was performed in 1 M KNO_3, and the applied potential on the pSi electrode was set at 0.8 V.

almost the same or even higher than that of a photograph of the stamp on paper. Oil, TPA, and TNT were also patterned on the porous silicon by the same method. In agreement with our expectations, pSi chips patterned with different chemicals displayed different ECL images (see Figure S4). The TPA pattern produced a positive image, whereas the TNT pattern generated a negative image. The ECL image produced on the oil-patterned pSi surface could shift from a negative to a positive image (see Figure S4 A,B). This phenomenon can be explained well by the dynamic ECL process of an oil-covered pSi surface (Figure 4): Initially, the ECL intensity of the oil-covered area is lower than that of the bare area of the pSi chip, and as a consequence, a negative image is generated. After a sufficient number of scanning cycles, the ECL intensity of the oil-covered area increases because of the dissolution of oil during voltammetric scanning, whereas the ECL intensity of the bare pSi decreases owing to the depletion of Si–H bonds. On this occasion, the conversion of gray-value contrast between the oil-covered and the bare area took place, thus leading to the conversion of the negative ECL image into a positive ECL image.

As a proof of principle, the visualization of LFPs was also demonstrated by using the ECL-based image-contrast tech-

nology. As we know, fingerprints result from the transfer of substances from the ridged epidermal skin of fingers to a surface during contact. Latent or invisible fingerprints are predominantly composed of the human skin secretions sweat (eccrine and apocrine) and sebum.[12] Up to now, secretions or exogenous chemicals present in fingerprints have been detected and mapped by Raman spectroscopy,[13] FTIR spectroscopy,[14] surface plasmon resonance,[15] and mass spectrometry.[16] Luminescence techniques, such as PL[17] and ECL,[8] have also been employed to image LFPs. However, current luminescence techniques usually require an additional luminophore and a coreactant. In the current approach, LFPs left on pSi can simply be visualized by ECL-based technology without the need for any molecular luminophore or coreactant. Impressions of fingerprints on a pSi surface may leave behind a unique spatially resolved chemical pattern. If a fingertip touches the pSi surface, the oily and tacky secretion on the ridge area will inevitably be transferred to the pSi surface to form an oil-based chemical pattern on pSi. For the same reason as described above, a negative ECL-based fingerprint image can be observed in the early stage (Figure 6A), in which the ECL intensity of the oil-covered part is lower than that of the bare area of pSi (Figure 1B). In further voltammetric cycles, the Si–H bond on the nonprotected area was quickly consumed, thus leading to the fading of ECL brightness on the bare area. In the meantime, the ECL intensity on oil-covered pSi gradually increased owing to the disruption of the oil layer during electrochemical scanning (Figure 1C). Consequently, the positive image of the fingerprint can be acquired at this stage (Figure 6B). To further confirm the transition of the fingerprint image from negative to positive, the ECL image of the selected rectangular area on both the negative and positive image was digitalized according to the relative gray value (see the Supporting Information), which was plotted against the CCD pixel number (Figure 6C). The result clearly indicates that a phase transition of the periodic gray-scale curve takes place and further confirms the shift of the ECL image from the negative to the positive mode.

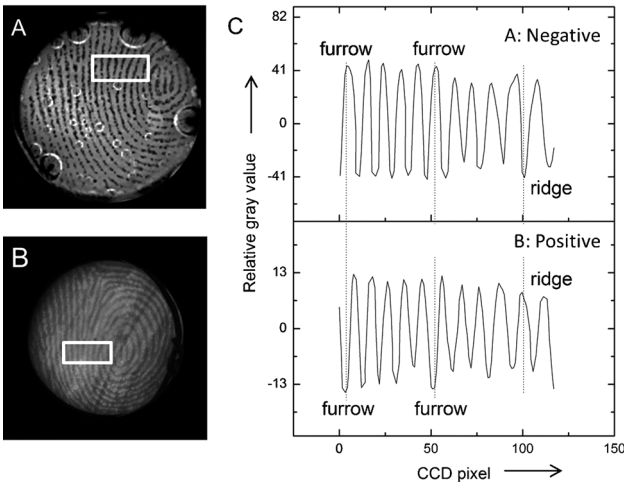

Figure 6. ECL images of LFPs on pSi as acquired with the image-contrast technology. A) Negative image of a LFP and B) positive image of a LFP. ECL images were measured in 1 M KNO_3 at an applied potential of 0.8 V. C) Cross-sectional relative gray values over 11 parallel ridges, as indicated by the white rectangles in (A) and (B).

Fingerprints not only consist of perspiration and natural secretion residues, but also contain exogenous components from the environment.[7] There is research interest in the identification of drugs, drug metabolites, and explosive residues in LFPs.[8,16,18] We believed that the ECL-based image-contrast technology could also be applied to detect those exogenous components in contact with a fingertip. To prove this concept, we also investigated the detection of explosive residues left on fingertips by using the established technology. If a fingertip touched the explosive trinitrotoluene (TNT), the TNT molecules would be absorbed on the fingertip. If this fingertip was then impressed on a pSi surface, partial transfer of the TNT molecules to the pSi surface would lead to a unique oily fingerprint. Owing to the ECL-quenching effect of TNT, the ECL-based fingerprint image may overlap with the quenching signal induced by TNT. We found that the TNT residue on a fingertip could be visualized and detected by the ECL-based image-contrast technology. Briefly, around 5 μL of a TNT solution (10 μg mL^{-1} in methanol) was dropped on half of a fingertip, which was impressed on a pSi chip 3 h later. For comparison, the same fingertip without TNT was also impressed on another pSi chip etched under the same conditions. ECL images of both pSi chips were acquired after 20 cycles of voltammetric scanning. At this stage, a positive fingerprint image was obtained on the control pSi chip (Figure 7A). In contrast, on the pSi impressed with a fingertip pretreated with a solution of TNT, part of the fingerprint image was significantly darker than the other area without TNT molecules. Clearly, the dark area is caused by the quenching effect of TNT on the ECL of pSi. The image of the TNT-containing fingerprint could also

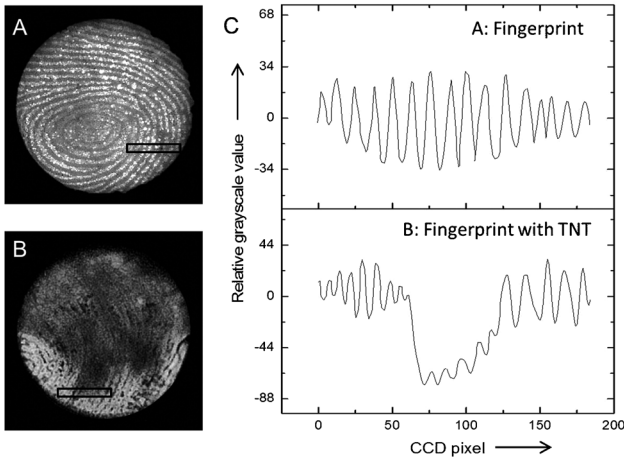

Figure 7. Detection of residues of TNT (10 μg mL^{-1} in methanol) on a fingerprint by using the ECL-based image-contrast technique. A) Positive ECL image of a LFP on pSi. B) ECL image of the LFP on pSi impressed with the same fingertip pretreated with TNT. C) Cross-sectional relative gray values over 15 parallel ridges within the area indicated by the black rectangles in (A) and (B). ECL measurements were performed in 1 M KNO_3 with an applied potential of 0.8 V.

be digitalized by plotting the relative gray value against the CCD pixel within a selected area (Figure 7C). The decreased gray value in parts of the selected region is apparently superposed on the periodic fingerprint gray-scale curve, thus indicating the quenching signal of the TNT molecules. The digitalized gray scale provides a possibility for quantification of the residual TNT molecules on a fingertip (see Figure S5). This detection technology will be very useful for identifying people who may have been in contact with explosives.

In summary, we have found that a dynamic ECL process can be perturbed by chemicals adsorbed on a pSi surface. Some chemicals may just block the electrochemical reaction on the pSi surface, thus resulting in a retarded activation process, whereas chemicals with electron-withdrawing or -donating ability will quench or enhance ECL intensity. On the basis of this mechanism, the visualization of chemical patterns with high resolution is possible with ECL-based image-contrast technology. The visualization of oily LFPs and explosive residues on the fingerprints has been demonstrated with this technology. As compared to ECL technology based on molecular luminescence, the technology proposed herein is simpler and does not need any coreactant. The application of this technology can potentially be extended to chemical-sensor arrays and the molecular imaging of tissue samples. If coupled with enzyme-amplification methods, the highly sensitive detection of target analytes and determination of their spatial distribution should be possible with the ECL-based image-contrast technology.

Received: May 4, 2014
Revised: June 23, 2014
Published online: July 17, 2014

Keywords: electrochemiluminescence · explosives detection · latent fingerprints · luminescence imaging · porous silicon

[1] a) S. Deng, H. Jiu, *Analyst* **2013**, *138*, 43 – 61; b) J. Li, S. Guo, E. Wang, *RSC Adv.* **2012**, *2*, 3579 – 3586.
[2] A. Gee, *J. Electrochem. Soc.* **1960**, *107*, 787 – 788.
[3] L. T. Canham, *Appl. Phys. Lett.* **1990**, *57*, 1046 – 1048.
[4] W. H. Green, E. J. Lee, J. M. Lauerhaas, T. W. Bitner, M. J. Sailor, *Appl. Phys. Lett.* **1995**, *67*, 1468 – 1470.
[5] Y. Mo, F. C. Li, B. Z. Zheng, S. L. Yang, H. Y. Yuan, Y. Guo, D. Xiao, *Electroanalysis* **2012**, *24*, 1887 – 1894.
[6] a) D. Andsager, J. Hilliard, J. M. Hetrick, L. H. Abuhassan, M. Plisch, M. H. Nayfeh, *J. Appl. Phys.* **1993**, *74*, 4783 – 4785; b) J. M. Lauerhaas, G. M. Credo, J. L. Heinrich, M. J. Sailor, *J. Am. Chem. Soc.* **1992**, *114*, 1911 – 1912; c) K. H. Li, C. Tsai, J. C. Campbell, M. Kovar, J. M. White, *J. Electron. Mater.* **1994**, *23*, 409 – 412; d) P. M. Fauchet, L. Tsybeskov, C. Peng, S. P. Duttagupta, J. von Behren, Y. Kostoulas, J. M. V. Vandyshev, K. D. Hirschman, *IEEE J. Sel. Top. Quantum Electron.* **1995**, *1*, 1126 – 1139.
[7] A. L. Beresford, A. R. Hillman, *Anal. Chem.* **2010**, *82*, 483 – 486.
[8] L. R. Xu, Y. Li, S. Z. Wu, X. H. Liu, B. Su, *Angew. Chem.* **2012**, *124*, 8192 – 8196; *Angew. Chem. Int. Ed.* **2012**, *51*, 8068 – 8072.
[9] a) J. M. Lavine, S. P. Sawan, Y. T. Shieh, A. J. Bellezza, *Appl. Phys. Lett.* **1993**, *62*, 1099 – 1101; b) R. C. Anderson, R. S. Muller, C. W. Tobias, *J. Electrochem. Soc.* **1993**, *140*, 1393 – 1396.
[10] S. Content, W. C. Trogler, M. J. Sailor, *Chem. Eur. J.* **2000**, *6*, 2205 – 2213.
[11] E. J. Lee, J. S. Ha, M. J. Sailor, *J. Am. Chem. Soc.* **1995**, *117*, 8295 – 8296.
[12] H. C. Lee, R. Ramotowski, R. E. Gaensslen, *Advances in Fingerprint Technology*, 2ednd edTaylor & Francis, Boca Raton, **2001**.
[13] E. Widjaja, *Analyst* **2009**, *134*, 769 – 775.
[14] M. Tahtouh, P. Despland, R. Shimmon, J. R. Kalman, B. J. Reedy, *J. Forensic Sci.* **2007**, *52*, 1089 – 1096.
[15] X. Shan, U. Patel, S. Wang, R. Iglesias, N. Tao, *Science* **2010**, *327*, 1363 – 1366.
[16] D. R. Ifa, N. E. Manicke, A. L. Dill, R. G. Cooks, *Science* **2008**, *321*, 805 – 805.
[17] a) H. Sohn, R. M. Calhoun, M. J. Sailor, W. C. Trogler, *Angew. Chem.* **2001**, *113*, 2162 – 2163; *Angew. Chem. Int. Ed.* **2001**, *40*, 2104 – 2105; b) Y. Li, L. R. Xu, B. Su, *Chem. Commun.* **2012**, *48*, 4109 – 4111.
[18] a) P. Hazarika, S. M. Jickells, K. Wolff, D. A. Russell, *Angew. Chem.* **2008**, *120*, 10321 – 10324; *Angew. Chem. Int. Ed.* **2008**, *47*, 10167 – 10170; b) X. Spindler, O. Hofstetter, A. M. McDonagh, C. Roux, C. Lennard, *Chem. Commun.* **2011**, *47*, 5602 – 5604.

